Near-infrared and upconversion properties of neodymium-doped $RE_{0.8}La_{0.2}VO_4$ (RE = Y, Gd) single-crystal fibres grown by the laser-heated pedestal growth technique

2002 J. Phys.: Condens. Matter 14 13889

(http://iopscience.iop.org/0953-8984/14/50/314)

INSTITUTE OF PHYSICS PUBLISHING JOURNAL OF PHYSICS: CONDENSED MATTER

J. Phys.: Condens. Matter **14** (2002) 13889–13897 PII: S0953-8984(02)39679-6

Near-infrared and upconversion properties of neodymium-doped $RE_{0.8}La_{0.2}VO_4$ (RE = Y, Gd) single-crystal fibres grown by the laser-heated pedestal growth technique

A S S de Camargo[1], **L A O Nunes, M R B Andreeta and A C Hernandes**

Instituto de Física de São Carlos, Universidade de São Paulo USP, CP 369, CEP 13566-590, São Carlos SP, Brazil

E-mail: andreasc@if.sc.usp.br (A S S de Camargo)

Received 18 July 2002
Published 6 December 2002
Online at stacks.iop.org/JPhysCM/14/13889

Abstract

Neodymium-doped $Y_{0.8}La_{0.2}VO_4$ and $Gd_{0.8}La_{0.2}VO_4$ single-crystal fibres were successfully grown by the laser-heated pedestal growth (LHPG) technique. The fibres were completely transparent and no dark inclusions were observed by optical microscopy. In the characterization process, microprobe Raman, optical absorption, fluorescence, lifetime, and gain-excited state absorption spectra were investigated in addition to upconversion measurements. The fibres' structural and spectroscopic properties are very similar to those of YVO_4 and $GdVO_4$ bulk laser crystals, with the advantageous characteristic of broadened spectral linewidths that facilitate the pumping of the 1064 nm emission by a diode laser. These fairly new crystal compositions, that can be grown in fast and economical processes, are potential candidates for use as compact laser-active media.

1. Introduction

Neodymium-doped orthovanadates such as YVO_4 and $GdVO_4$ have motivated several studies due to their application as efficient diode-pumped laser-active media at 1064 nm with better properties than YAG:Nd^{3+} [1–6]. Such properties include higher optical absorption and emission cross-sections and higher Nd^{3+} doping incorporation [2–4]. Also, because these vanadates are anisotropic crystals, their laser transitions are polarized, and that represents an another advantage over YAG:Nd^{3+} for frequency-doubling systems. Most of the structural and spectroscopic investigations of YVO_4 and $GdVO_4$ have been done on large crystals grown mainly by the Czochralski method; however, the increasing demand for compactness of optical

[1] Author to whom any correspondence should be addressed.

devices has recently raised interest in single-crystal fibres (SCFs) [7, 8]. Among the techniques that can be used for the production of such materials, the laser-heated pedestal growth (LHPG) technique has proved to be very efficient and interesting due to its low-cost operation and the possibility of fibre growth in much faster processes than the usual ones. Unlike in other methods, the heating element in LHPG is a CO_2 laser and that is what makes the technique economically interesting, since the need for special crucibles (Ir, Pt, Mo) for high-temperature growth is eliminated.

Growth of YVO_4 and $GdVO_4$ single crystals has proved to be a difficult task—not only by LHPG, but also using other techniques. Apparently, oxygen deficiencies cause valence changes of vanadium ions during growth and that results in the inclusion of dark phases that compromise the optical quality of the crystals [9, 10]. Moreover, the high melting points of these compounds ($\sim$2000 °C) add further difficulties to their growth. In the case of LHPG, the melting zones are usually very turbulent and, due to the high axial temperature gradient, it is difficult to control the diameters of the fibres, and unwanted strain fields and cracks are often generated. The conditions are even worse for $GdVO_4$ because of its helicoidal growth. In view of this, several attempts have been made to improve the growth conditions of these compounds, including changes in precursors and stoichiometry, growth atmosphere, pulling rates, and post growth thermal treatments [11–13]. More recently, we have made a contribution by reporting on the successful employment of an isostatic oxygen atmosphere (5–10 atm) during the melt and pulling processes of LHPG to obtain transparent YVO_4:Nd^{3+} fibres at high pulling rates ($\sim$0.5 mm min^{-1}) [13].

Considering Nd^{3+} laser emission at 1064 nm ($^4F_{3/2} \rightarrow {}^4I_{11/2}$ transition), efforts have been made to optimize the pumping of the level $^4F_{3/2}$ by powerful and inexpensive diode lasers at around 808 nm. Since the typical linewidth of these lasers is 2–3 nm, which is wider than the absorption band of most neodymium-doped crystals, temperature control of the diode is often needed for perfect tuning [14]. To avoid this inconvenience and increase the tolerance in the pump wavelength selection, a controlled disorder can be introduced in the crystals in order to broaden spectral lines. In YVO_4 and $GdVO_4$ crystals, La^{3+} ions can be used for that purpose while substituting Y^{3+} and Gd^{3+} [14, 15]. Bulk crystals of $Gd_{1-x}La_xVO_4$:Nd^{3+}, grown by the Czochralski method, have been investigated [15–17] and present the same structure (for $x \leqslant 0.58$ mol% La^{3+}), and laser efficiency comparable to that of $GdVO_4$:Nd^{3+}, in addition to larger spectral linewidths [16]. Also, one interesting thing to be noted is the significant improvement of growing conditions as a function of La^{3+} inclusion. Although similar behaviour is expected for $Y_{1-x}La_xVO_4$:Nd^{3+}, this crystal composition has not been explored yet and neither has there been any study of LHPG-grown SCFs.

The aim of this work was to obtain undoped or Nd^{3+}-doped $Gd_{0.8}La_{0.2}VO_4$ and $Y_{0.8}La_{0.2}VO_4$ SCFs by LHPG and characterize them by microprobe Raman, optical absorption, fluorescence in the near-infrared region, upconversion, and excited state lifetime measurements. In addition, excited state absorption (ESA) spectra were obtained in order to evaluate the influence of this process on the effective infrared emission cross-sections of Nd^{3+} in these new crystal host compositions. The yellow-to-blue upconversion is also generated by an ESA mechanism and its observation also indicates the potentiality of the fibres for obtaining emission in the blue region [18, 19]. The spectroscopic characterization was done in comparison to spectra of commercial bulk laser crystals.

2. Experimental details

Undoped or Nd^{3+}-doped fibres (0.5, 1.0, and 5.0 mol%) were prepared from cylindrical pedestals produced by mixing stoichiometric amounts of optical grade Y_2O_3, Gd_2O_3, La_2O_3,

V_2O_5, and Nd_2O_3 with an organic ligand [20]. The pedestals were used as both seed and feed rods during the melt and pulling processes. Microprobe Raman spectra were obtained for undoped samples with non-polarized excitation of an argon-ion laser at 514.5 nm. Light focusing was monitored by a CCD camera and controlled by an objective lens. The signal was filtered by a triple monochromator (0.6 m) and collected by a CCD. Absorption measurements of Nd^{3+}-doped fibres were made using a Nicolet Magna IR 850 spectrophotometer equipped with a Si detector and quartz beam splitter. Fluorescence spectra were obtained by exciting the samples with a diode laser at 808 nm. The signal was filtered by a 0.3 m monochromator, collected by an InGaAs detector, and amplified by a lock-in system. The curves for the fluorescence time decay from the level $^4F_{3/2}$ were measured using an OPO laser at 800 nm and from them it was possible to obtain the average $1/e$ lifetime values.

The ESA measurements were performed using a pump–probe experimental set-up as described in [21]. The samples were pumped by a 14 Hz modulated Ti:sapphire laser at 808 nm and the probe radiation was provided by a broadband tungsten lamp modulated at 600 Hz; the signal was filtered by a 0.3 m monochromator and collected by a Ge detector. By taking the normalized difference between the transmitted intensities I_p, for the pumped crystal sample, and I_u, for the unpumped sample, one can relate the ground state absorption σ_{GSA}, the stimulated emission σ_{SE}, and the ESA σ_{ESA} in the following way:

$$\frac{I_p(\lambda) - I_u(\lambda)}{I_p(\lambda)} = n_e \zeta L \left[\sigma_{GSA}(\lambda) + \sum_i \left(\frac{n_i}{n_e} \right) (\sigma_{SE,i} + \sigma_{ESA,i}) \right] \tag{1}$$

where n_e is the overall excited population, ζ is the amplification factor of the lock-in, and L is the sample thickness; n_i/n_e is the ratio of the population in level i to the total population of excited ions. The spectra can be calibrated in regions where only ground state absorption and stimulated emission are present and ESA is not expected. Absorption cross-sections are determined from independent measurements and the emission cross-sections around 1064 nm were determined by the Fuchtbauer–Lundenburg expression [22] that relates the emission lineshape and emitting level lifetime to the emission cross-sections. Because there is not ESA at 1064 nm and the only metastable level is $^4F_{3/2}$, the ratio n_i/n_e is 1 and therefore the calibrations were done by imposing equality of the stimulated emission cross-sections of the $^4F_{3/2} \rightarrow {}^4I_{11/2}$ transition and the $(I_p - I_u)/I_p$ spectra. Absorption and ESA measurements were obtained in π-polarization ($E \parallel c$).

Upconversion spectra were obtained with excitation from a dye laser at around 590 nm. The signal was filtered by a double monochromator and detected by a RCA31034 photomultiplier.

3. Results

The undoped or Nd^{3+}-doped single-crystal fibres of $Y_{0.8}La_{0.2}VO_4$ and $Gd_{0.8}La_{0.2}VO_4$, with dimensions of 400–600 μm diameter and 1–2 cm length, were successfully grown by LHPG. The fibres were completely transparent and no dark inclusions were observed by optical microscopy. The undoped samples are colourless but the doped ones present a light blue coloration that is slightly enhanced by increasing the Nd^{3+} concentration. The structure of $REVO_4$ (RE = Ce–Lu, Y, and Sc) was confirmed by x-ray diffraction pattern analysis of all samples [23]. Figure 1 presents the Raman spectra of: (a) $Y_{0.8}La_{0.2}VO_4$ and (c) $Gd_{0.8}La_{0.2}VO_4$ single-crystal fibres, in comparison to those of: (b) YVO_4 and (d) $GdVO_4$ bulk single crystals grown by the Czochralski method.

The room temperature ground state absorption spectra of $Y_{0.8}La_{0.2}VO_4$ and $Gd_{0.8}La_{0.2}VO_4$ SCFs doped with 1.0 mol% Nd^{3+} in the range of 670–930 nm are shown in figure 2, in

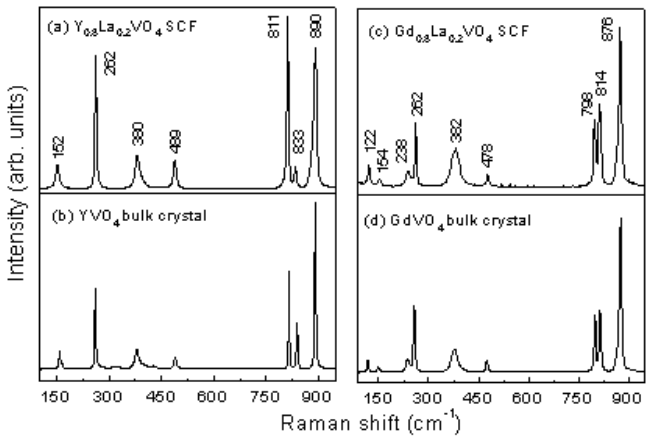

Figure 1. Non-polarized microprobe Raman spectra of undoped fibres: (a) $Y_{0.8}La_{0.2}VO_4$ and (c) $Gd_{0.8}La_{0.2}VO_4$; in comparison with bulk crystals: (b) YVO_4 and (d) $GdVO_4$ ($\lambda_{exc} = 514.5$ nm).

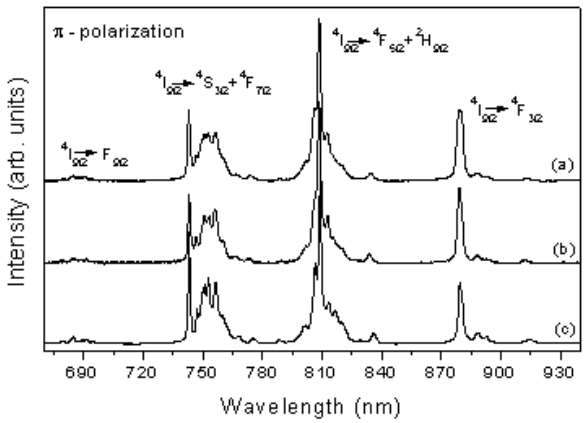

Figure 2. Room temperature ground state absorption spectra of single-crystal fibres doped with 1.0 mol% Nd^{3+}: (a) $Y_{0.8}La_{0.2}VO_4$ and (b) $Gd_{0.8}La_{0.2}VO_4$; in comparison with (c) YVO_4 bulk single crystal doped with 1.0 mol% Nd^{3+}. The spectra were obtained in π-polarization.

comparison to the spectrum of the YVO_4:Nd^{3+} commercial bulk laser crystal. The spectra were obtained under π-polarization excitation, which yields higher cross-sections, as in the ESA measurements. Representative fluorescence spectra in the range of 820–1440 nm are presented in figure 3. The transitions from the level $^4F_{3/2}$ to $^4I_{13/2}$, $^4I_{11/2}$ and $^4I_{9/2}$ (corresponding to the observed bands) are indicated in the partial energy level diagram of the figure. Figure 4 shows the gain-ESA spectra of $Y_{0.8}La_{0.2}VO_4$ and $Gd_{0.8}La_{0.2}VO_4$ SCFs doped with 5.0 mol%. In the range of 950–1450 nm no GSA bands are observed and the stimulated emission and ESA peaks from the level $^4F_{3/2}$ are indicated. Finally, figure 5 presents the upconversion spectra of the fibres in comparison to that of bulk YVO_4:Nd^{3+}. The ESA responsible for the excitation of $^2P_{3/2}$ and transitions from this level are indicated in the partial energy level diagram in the inset.

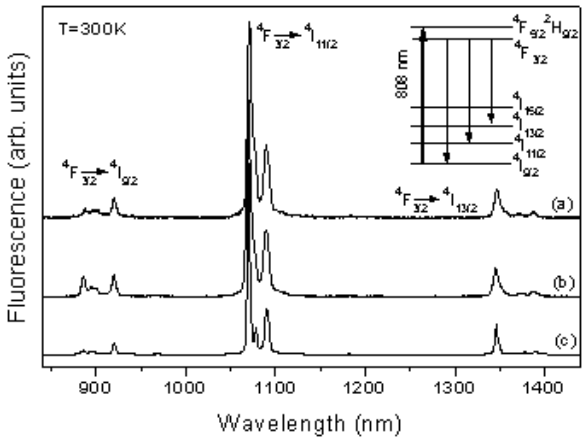

Figure 3. Fluorescence spectra of single-crystal fibres doped with 1.0 mol% Nd^{3+}: (a) $Y_{0.8}La_{0.2}VO_4$ and (b) $Gd_{0.8}La_{0.2}VO_4$ in comparison with bulk crystal YVO_4:Nd^{3+} (c). The inset shows the partial energy level diagram indicating the radiative transitions from $^4F_{3/2}$.

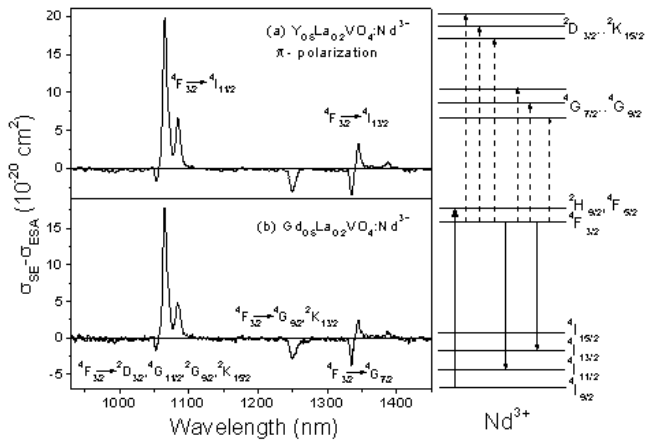

Figure 4. Gain-ESA spectra (π-polarization) of single-crystal fibres doped with 5.0 mol% Nd^{3+}: (a) $Y_{0.8}La_{0.2}VO_4$:Nd^{3+}; (b) $Gd_{0.8}La_{0.2}VO_4$:Nd^{3+}. The transitions from the level $^4F_{3/2}$ are indicated in the partial energy level diagram.

4. Discussion

The introduction of La^{3+} was very beneficial for the conditions of growth of the fibres by LHPG without the need for an O_2 atmosphere [13]. In the beginning, the melt and pulling processes are very turbulent—similarly to the cases for YVO_4 and $GdVO_4$—but after some minutes, the growth becomes much more stable, while a decrease of $\sim$300 °C in the temperature of the liquid zone is verified to occur. To investigate these changes, the fibres' molten zones were investigated by EDX analysis as a function of time and it was verified that at the beginning of the growth there is a deficiency of lanthanum in them, whereas after stabilization they become La^{3+} enriched. The modification in composition also favoured transparency of the fibres to the detriment of the dark phases previously observed in YVO_4:Nd^{3+} due to vanadium oxide evaporation [13]. One possible explanation is based on the fact that since La^{3+} has a larger ionic

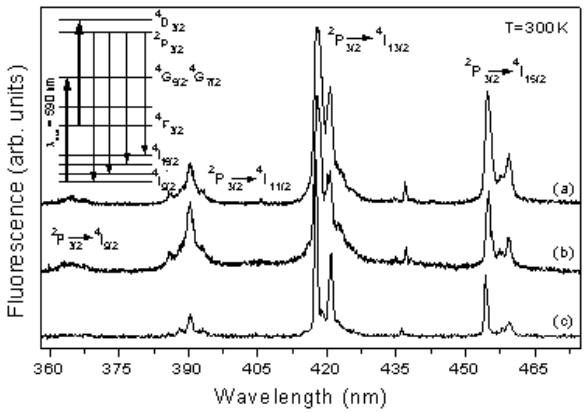

Figure 5. Upconversion spectra of single-crystal fibres doped with 1.0 mol% Nd^{3+}: (a) $Y_{0.8}La_{0.2}VO_4$ and (b) $Gd_{0.8}La_{0.2}VO_4$ in comparison with bulk crystal YVO_4:Nd^{3+} (1.0 mol%) (c), obtained with $\lambda_{exc} = 590$ nm. The transitions corresponding to the bands observed are indicated in the partial energy level diagram in the inset.

radius than Gd^{3+} and Y^{3+} [14], the lattice constants of $Gd_{0.8}La_{0.2}VO_4$ ($a = b = 0.7239$ nm and $c = 0.6360$ nm) are slightly larger than those of $GdVO_4$ ($a = b = 0.721\,26$ nm and $c = 0.634\,83$ nm) [17] and that may be enough to introduce lattice distortions that could cause a decrease in the site size, favouring the presence of V^{5+}, with smaller ionic radii than V^{3+} and V^{4+}, which are responsible for the formation of dark phases.

The tetragonal zircon-type structure of $REVO_4$, space group $I4_1/amd$, was confirmed by analysis of the fibres' diffraction patterns [23] and the disordering effect introduced by La^{3+} is clearly evidenced in figures 1(a) and (c) by the broadening of Raman lines in comparison to those of the bulk crystals ((b) and (d)). The bands corresponding to frequencies up to 200 cm^{-1} are attributed to external modes of vibration of VO_4^{3-} and Ln^{3+} ions, and those in the range of 200–1000 cm^{-1} correspond to internal modes of VO_4^{3-} [24, 25]. In accordance with previous reports for Nd^{3+}-doped $Gd_{0.8}La_{0.2}VO_4$ bulk crystals [14, 17], line broadening is also observed in the fibres' ground state absorption spectra, in figures 2(a) and (b), in comparison to that of the YVO_4:Nd^{3+} bulk crystal, figure 2(c). The absorption bands at around 808 nm in (a) and (b) present full width at half-maximum (FWHM) of 2.8 and 3.7 nm respectively, whereas that of YVO_4:Nd^{3+} bulk crystal in (c) is approximately 2 nm. That is in accordance with the observations made by Ostroumov *et al* [14] for $Gd_{0.5}La_{0.5}VO_4$:Nd^{3+} bulk crystal, although Wang *et al* [15] concluded that, contrary to the case for 50 mol% La^{3+} addition in Nd:$GdVO_4$, the percentage of 20 mol% would not result in broadening of the absorption band as compared to that for Nd:$GdVO_4$ crystal. We have also investigated the composition with 40 mol% La^{3+}, but no appreciable differences between it and the 20 mol% one were detected.

At 1064 nm the fluorescence is constituted by unresolved peaks, as can be noted in the fibre spectra of figures 3(a) and (b), and the FWHM is approximately 5.4 nm for both. These lines are slightly narrowed in the spectra obtained at $T = 5$ K, but even so, there is still an overlap of different lines originating from the two $^4F_{3/2}$ Stark levels. Considering the $^4F_{3/2} \rightarrow {}^4I_{9/2}$ transition, one can see only four lines in figure 3, since the splitting is small ($\sim$25 cm^{-1}) and the lines are also broadened. The transition $^4F_{3/2} \rightarrow {}^4I_{15/2}$ is not observable because it is outside the measured spectral range. The radiative lifetime values of $^4F_{3/2}$ obtained from the fluorescence decay curves at 1064 nm are 90 and 92 μs for the 0.5% Nd^{3+}-doped $Y_{0.8}La_{0.2}VO_4$ and $Gd_{0.8}La_{0.2}VO_4$ samples respectively. However, for the fibres with 5.0 mol% doping the

lifetimes drop to ∼25 μs due to an increase in the probability of energy transfer processes such as the cross-relaxation $^4F_{3/2}$, $^4I_{9/2} \rightarrow {}^4I_{15/2}$, $^4I_{15/2}$. Using the radiative lifetime values and the experimental branching ratios $\beta_{(J;J')}$, it was possible to obtain the emission probabilities $A_{(bJ';aJ)}$, and from the emission spectra we calculated the emission peak cross-sections at 1064 and 1342 nm according to [26, 27]

$$\sigma(J;J') = \frac{\lambda_p^4}{8\pi cn^2\,\Delta\lambda_{ef}} A[(bJ';aJ)] \tag{2}$$

where λ_p is the peak wavelength and $\Delta\lambda_{ef}$ is the ratio between the band area and its peak intensity, c is the speed of light, and n is the refractive index. The values of the emission cross-sections were found to be very similar for the two crystal compositions. For $Y_{0.8}La_{0.2}VO_4$:Nd^{3+}, $\sigma_{SE}^{1064\,nm} = 30 \times 10^{-20}$ and $\sigma_{SE}^{1342\,nm} = 17 \times 10^{-20}$ cm^2, whereas for $Gd_{0.8}La_{0.2}VO_4$:Nd^{3+} values of $\sigma_{SE}^{1064\,nm} = 26 \times 10^{-20}$ and $\sigma_{SE}^{1342\,nm} = 12.5 \times 10^{-20}$ cm^2 were obtained in accordance with the report by Ostroumov *et al* [14] for $Gd_{0.5}La_{0.5}VO_4$:Nd^{3+}. These values are significantly smaller than those reported for YVO_4:Nd^{3+} (120×10^{-20} and 45×10^{-20} cm^2 [30]) and $GdVO_4$:Nd^{3+} (76×10^{-20} and 18×10^{-20} cm^2 [2]) due to the inhomogeneous broadening, but comparable to those for YAG:Nd^{3+}.

Figure 4 presents the gain-ESA spectra of the fibres doped with 5.0 mol%. In this spectral range, one can observe the stimulated emissions at 1064 and at 1342 nm corresponding to the transitions from $^4F_{3/2}$ to levels $^4I_{11/2}$ and $^4I_{13/2}$, and also the ESA transitions from $^4F_{3/2}$ to the groups of levels $^4G_{9/2}$, $^4G_{11/2}$, $^2K_{15/2}$ (from 980 to 1063 nm), $^2G_{9/2}$, $^2K_{13/2}$ (around 1260 nm) and to level $^4G_{7/2}$ (around 1340 nm) as shown in the partial energy level diagram. As can be noted, the spectra in (a) and (b) are very similar but the peak emission cross-sections are smaller than the calculated ones due to low resolution of the experimental apparatus. Therefore, these values cannot be taken as absolute, but even so, the SE/ESA intensity ratios around 1064 and 1342 nm are similar to those observed by Fornasiero *et al* [30] for YVO_4:Nd^{3+} and $GdVO_4$:Nd^{3+} crystals. The maximum ESA cross-section at 1056 nm is 1×10^{-20} cm^2 and even if there is an overlap of a wing of this transition (with smaller σ_{ESA}) with the stimulated emission at 1064 nm, it is evident that the ESA loss at this wavelength is negligible in comparison to the emission cross-section of at least 18×10^{-20} cm^2. Therefore the efficiency of the laser transition at 1064 nm should not be compromised by ESA transitions. The laser line at 1342 nm, however, lies much closer to a strong ESA transition and, considering its linewidth (typically 2 nm), we can infer that the laser performance at this wavelength is strongly degraded due to spectral overlap (see the spectra in figure 3 for comparison).

Finally, the upconversion spectra of the fibres and bulk crystal presented in figure 5 also indicate the possibility of ESAs from the level $^4F_{3/2}$ (under 590 nm excitation) that promote electrons to higher-lying levels in the violet spectral region. The upconversion process happens via a sequential two-step absorption of the yellow pump photons; that is, the absorption of a first photon excites electrons from the ground state $^4I_{9/2}$ to $^2H_{11/2}$ and, after non-radiative relaxation to intermediate, metastable $^4F_{3/2}$ takes place, a second photon absorption excites the upper level $^4D_{3/2}$. Because the lifetime of this level is very short, it relaxes to lower-lying $^2P_{3/2}$ from which the upconversion emissions to levels $^4I_{9/2}$, $^4I_{11/2}$, $^4I_{13/2}$, and $^4I_{15/2}$ at 365, 390, 420, and 460 nm are observed, according to the inset of figure 5. In fact, the curve of the upconversion intensity as a function of excitation power has a slope of ∼2, as is expected for an ESA pumping. Measurements as a function of time were also done to investigate the possibility of photon avalanche in these systems, but this regime of excitation was not observed.

5. Conclusions

Neodymium-doped or undoped $Y_{0.8}La_{0.2}VO_4$ and $Gd_{0.8}La_{0.2}VO_4$ single-crystal fibres were successfully grown by the LHPG technique and characterized by Raman, optical absorption, fluorescence, upconversion, and lifetime measurements. The structural and spectroscopic results are very similar to those obtained for bulk YVO_4 and $GdVO_4$ crystals, except for the broadening of the absorption and emission lines due to the introduction of 20 mol% La^{3+} to substitute for Gd^{3+} and Y^{3+} ions. The line broadening can be an advantageous characteristic when it comes to diode pumping at 808 nm without the need for temperature control of the diode. For both compositions, the presence of La^{3+} also improved the growing conditions and optical quality of the fibres as a result of better stability of the molten zone. The gain-ESA spectra of the fibres are also very similar to those of $GdVO_4$ and YVO_4 crystals, indicating that the introduction of La^{3+} does not increase ESA probabilities at around 1060 and 1340 nm in relation to the stimulated emissions, although the latter's cross-sections are decreased due to inhomogeneous spectral broadening. It was also concluded that the upconversion pumping mechanism of levels lying in the violet spectral region can potentially be used for the construction of compact lasers in the blue region. Although the spectroscopic properties of rare-earth vanadates have been extensively explored, the significant contribution of this work is to present a compositional change that allows crystal growth using an economically interesting and time-saving technique with optical quality comparable to that of Czochralski-grown crystals. Moreover, the anisotropic nature of these crystal fibres is very interesting as regards second-harmonic generation.

Acknowledgments

This work was supported by CNPq (Conselho Nacional de Desenvolvimento Cientifico e Tecnológico), CAPES (Coordenação de Aperfeiçoamento de Pessoal de Nível Superior) and FAPESP (Fundação de Amparo a Pesquisa do Estado de São Paulo).

References

[1] O'Connor J R 1966 *Appl. Phys. Lett.* **9** 407
[2] Jensen T, Ostroumov V G, Meyn J-P, Huber G, Zagumennyi A I and Shcherbakov I A 1994 *Appl. Phys.* B **58** 373
[3] Agnesi A, Penachio C, Realli G C and Kubecek V 1997 *Opt. Lett.* **22** 1645
[4] Zhang H J, Zhu L, Meng X L, Yang Z H, Wang C Q, Yu W T, Chow Y T and Lu M K 1999 *Cryst. Res. Technol.* **34** 1011
[5] Zhang H J, Liu J, Wang J, Wang C, Zhu L, Shao Z, Meng X, Hu X, Jiang M and Chow Y T 2002 *J. Opt. Soc. Am.* B **19** 18
[6] Shimamura K, Uda S, Kochurikhin V V, Taniuchi T and Fukuda T 1996 *Japan. J. Appl. Phys.* **35** 1832
[7] Zayhowski J J 1999 *Opt. Mater.* **11** 255
[8] Pavel N, Taira T and Furuhata M 1998 *Opt. Laser Technol.* **30** 275
[9] Erdei S and Ainger F W 1993 *J. Cryst. Growth* **128** 1025
[10] Huang C-H and Chen J-C 2001 *J. Cryst. Growth* **229** 184
[11] Goutadier C, Ermeneux F S, Cohen-Adad M T, Moncorgé R, Betinelli M and Cavalli E 1998 *Mater. Res. Bull.* **33** 1457
[12] Huang C-H and Chen J-C 2000 *J. Cryst. Growth* **211** 237
[13] Ardila D R, de Camargo A S S, Andreeta J P and Nunes L A O 2001 *J. Cryst. Growth* **233** 253
[14] Ostroumov V G, Huber G, Zagumennyi A I, Zavartsev Y D, Studenikin P A and Shcherbakov I A 1996 *Opt. Commun.* **124** 63
[15] Wang C Q, Zhang H J, Chow Y T, Liu J H, Zhu L, Wang J Y, Meng X L and Gambling W A 2001 *Opt. Laser Technol.* **33** 439

[16] Zhang H, Meng X, Zhu L, Wang C, Wang P, Zhang H, Chow Y T and Dawes J 1998 *J. Cryst. Growth* **193** 370
[17] Zhang H, Wang C, Zhu L, Liu X, Zhang G, Yu W, Meng X and Chow Y T 2002 *J. Mater. Res.* **17** 556
[18] Joubert M F 1999 *Opt. Mater.* **11** 181
[19] Risk W P 1990 *Opt. Photon. News* **May** 10
[20] Andreeta M R B, Hernandes A C, Guevara J A, Cuffini S L and Mascarenhas Y P 1999 *J. Cryst. Growth* **200** 621
[21] Koetke J and Huber G 1995 *Appl. Phys.* B **61** 151
[22] Miniscalco W J and Quimby R S 1991 *Opt. Lett.* **16** 258
[23] JCPDS—International Center for Diffraction Data file No 17 p341
[24] Miller S E, Caspers H H and Rast H E 1968 *Phys. Rev.* **168** 964
[25] Xia H R, Hu L, Zou J, Li L, Yu H, Meng X, Zhu L and Yu W 1998 *Cryst. Res. Technol.* **33** 807
[26] Judd B R 1962 *Phys. Rev.* **127** 750
[27] Ofelt G S 1962 *J. Chem. Phys.* **37** 511
[28] Tucker A W, Birnbaum M, Fincher C L and Erler J W 1977 *J. Appl. Phys.* **48** 4907
[29] Xia H R, Meng X L, Guo M, Zhu L, Zhang H J and Wang J Y 2000 *J. Appl. Phys.* **88** 5134
[30] Fornasiero L, Kück S, Jensen T, Huber G and Chai B H T 1998 *Appl. Phys.* B **67** 549